

# RSC Advances



This is an *Accepted Manuscript*, which has been through the Royal Society of Chemistry peer review process and has been accepted for publication.

*Accepted Manuscripts* are published online shortly after acceptance, before technical editing, formatting and proof reading. Using this free service, authors can make their results available to the community, in citable form, before we publish the edited article. This *Accepted Manuscript* will be replaced by the edited, formatted and paginated article as soon as this is available.

You can find more information about *Accepted Manuscripts* in the [Information for Authors](#).

Please note that technical editing may introduce minor changes to the text and/or graphics, which may alter content. The journal's standard [Terms & Conditions](#) and the [Ethical guidelines](#) still apply. In no event shall the Royal Society of Chemistry be held responsible for any errors or omissions in this *Accepted Manuscript* or any consequences arising from the use of any information it contains.

**Complexation of Triblock Reverse Copolymer 10R5 with Surface Active Ionic Liquids in Aqueous Medium: A Physico-chemical Study**

**Renu Sharma, Tejwant Singh Kang,\* Rakesh Kumar Mahajan\***

\*Department of Chemistry, UGC-Centre for Advanced Studies-I, Guru Nanak Dev University, Amritsar-143005, India

RSC Advances Accepted Manuscript

*\*To whom correspondence should be addressed:*

*e-mail:* [rakesh\\_chem@yahoo.com](mailto:rakesh_chem@yahoo.com); [tejwantsinghkang@gmail.com](mailto:tejwantsinghkang@gmail.com); Fax: +91 183 2258820

**Abstract**

A comprehensive study on the interactions of surface active ionic liquids (SAILs) 1-alkyl-3-methyl imidazolium chlorides,  $[C_n\text{mim}][\text{Cl}]$ , where  $n = 8, 10, \text{ and } 12$ , with a triblock reverse copolymer, 10R5,  $[(\text{PPO})_8-(\text{PEO})_{22}-(\text{PPO})_8]$  has been performed using various physico-chemical techniques viz. surface tension, conductivity, isothermal titration calorimetry (ITC), turbidity, fluorescence spectroscopy, and dynamic light scattering (DLS). The interactions between triblock reverse copolymer with SAILs have been emphasized in terms of three concentration regions due to different modes of interactions between them whereas the previous studies reported that interactions between cationic surfactants and triblock copolymers are moderately weak. Different transitions corresponding to different stages of interactions of 10R5 with SAILs are observed from different techniques. Various thermodynamic parameters are calculated using conductivity and ITC measurements, whereas fluorescence studies have provided useful information about the polarity of the cybotactic region of probe in the complexes formed by 10R5 and SAILs. The size of polymer-SAIL complexes have been investigated using dynamic light scattering and ITC measurements. The results obtained from different techniques have been correlated with each other to get a concise picture regarding the type of interactions prevailing between polymer and SAILs.

---

**Keywords:** Surface active ionic liquids, Triblock copolymer 10R5, Micellization, Thermodynamics, Hydrophobicity, Isothermal titration calorimetry.

## 1. Introduction

Water soluble triblock copolymers of poly (ethylene oxide) (PEO) and poly (propylene oxide) (PPO) in the forms of PEO-PPO-PEO (normal pluronics) and PPO-PEO-PPO (reverse pluronics) are a series of high molecular weight nonionic surfactants comprising of hydrophilic PEO block and hydrophobic PPO block. Triblock copolymers have attracted much attention in the past few years due to their wide spread applications in diverse fields [1-4]. The flexible molecular framework of pluronics makes them special to undergo self-aggregation in aqueous solution above their critical micelle concentration (*cmc*) at and above their critical micelle temperature (*cmt*) [5, 6]. The reverse pluronics exhibit different characteristics in the aqueous solution as compared to normal pluronics. The other area of immediate interest is the utilization of these pluronics in conjunction with surfactants to achieve better colloidal properties. In this regard, the micellization of triblock copolymers in the presence of surfactants [7, 8], organic additives [9] and inorganic salts [10] have been reported. Our own research group has performed numerous investigations related to the interactions of triblock copolymers and ionic surfactants [11-13]. In this regard, O. Ortona *et al.*, [14] have investigated the interactions of normal PE6200 and reverse 25R4 pluronics with anionic sodium decylsulfate, C<sub>10</sub>OS, cationic decyltrimethyl ammonium bromide, C<sub>10</sub>TAB and nonionic pentaethylene glycol monodecyl ether, C<sub>10</sub>E<sub>5</sub> surfactants using various techniques. Both pluronics have been found to interact strongly with anionic surfactant, feebly with cationic and unresponsive in the presence of nonionic surfactants. J. Mata *et al.*, [15] have investigated the aggregation behavior of triblock copolymer P105 with sodium dodecyl sulphate (SDS) and dodecyltrimethylammonium bromide (DTAB) in aqueous and salt solutions. They concluded that addition of ionic surfactants in low concentration to micellar solution of P105 cause demicellization. A few reports are also available for the interactions between reverse pluronics and ionic surfactants [14, 16-18]. Recently, S. P. Moulik *et al.*, [17] have reported the solution behavior of normal L44 (L) and reverse 10R5 (R) pluronics, individually and in binary mixture exploiting various techniques. In another report, anionic surfactant sodium N-dodecanoylsarcosinate (SDDS) has been found to bind more strongly to R than L due to difference in the arrangement of PPO/PEO segments of pluronics used [18].

On the other hand, in the past few years, ionic liquids (ILs) have attracted a great interest owing to their unique physico-chemical properties [19-22] and find numerous applications in different areas [23-30]. One of the important classes of ILs is surface active ionic liquids (SAILs), which are structurally similar to conventional ionic surfactants. Till date, a variety of SAILs have been reported for their aggregation behavior in aqueous medium [31-34]. The nature of cationic/anionic head group, counter-ion and the length of alkyl chain has been found to affect their aggregation behavior [35-38]. In some cases, SAILs have been found to exhibit better surface active properties as compared to conventional ionic surfactants [39, 40]. Amphiphilic nature of these SAILs can be varied by plethora of possible ion-pair combinations that offer an unparalleled ability to tune both physical and chemical properties for specific applications. Utilizing the surface active properties of SAILs, many research groups have investigated the interactions of SAILs with a variety of biopolymers like gelatin, agarose, chitosan and bovine serum albumin etc. to get better colloidal properties [41-45]. However, with few exceptions, the detailed investigations on interactions of SAILs with block copolymers in aqueous medium are much lacking [46-48]. Further, the novelty of the work lies in the fact that there exists no report shedding light on interactions between SAILs and reverse pluronics, in literature.

In the present work, we have focused on the interactions between reverse pluronic 10R5 and SAILs: 1-alkyl-3-methyl imidazolium chlorides,  $[C_n\text{mim}][\text{Cl}]$ , where  $n = 8, 10, \text{ and } 12$ . The interactional behavior of SAILs with block copolymer have been investigated by surface tension, conductivity, isothermal titration calorimetry (ITC), turbidity, fluorescence, and dynamic light scattering (DLS) techniques. Various surface parameters like critical micelle concentration ( $cmc$ ) surface tension at  $cmc$  ( $\gamma_{cmc}$ ), Gibbs surface excess ( $\Gamma_{\text{max}}$ ), minimum area per molecule ( $A_{\text{min}}$ ) have been calculated using surface tension data. Thermodynamic parameters of micellization *i.e.* Gibbs free energy ( $\Delta G_{\text{mic}}$ ), enthalpy ( $\Delta H_{\text{mic}}$ ) and entropy ( $\Delta S_{\text{mic}}$ ) of micelle formation have been calculated using conductivity and ITC measurements. Fluorescence measurements have provided information about  $cmc$ , polarity and the aggregation number of the aggregates of SAILs in the absence and presence of polymer 10R5. The variation in size of the aggregates formed by SAILs and polymer have been observed using DLS technique.

## 2. Experimental section

### 2.1. Materials

The surface active ionic liquids (SAILs), 1-alkyl-3-methylimidazolium chloride  $[C_n\text{mim}][\text{Cl}]$  where  $n = 8, 10,$  and  $12$  were prepared by the procedure mentioned elsewhere in the literature [40] and then characterized by  $^1\text{H}$  NMR technique. 1-methyl imidazole, 1-chlorooctane, 1-chlorodecane, 1-chlorododecane, reverse pluronic 10R5 and fluorescence probe pyrene with 98% purity were purchased from Sigma Aldrich. The molecular structures of SAILs and polymer are shown in Scheme 1 (a-b). Cetylpyridinium chloride (CPC) with 98 % purity was purchased from Lancaster Synthesis, UK. All the materials were used as received. All the solutions were prepared in double distilled deionized water. A sartorius analytical balance with a precision of  $\pm 0.0001$  g was used for weighing purpose.

### 2.2. Methods

For all the measurements, titration method was used keeping the concentration of polymer, 10R5 constant at  $0.5 \text{ mmol dm}^{-3}$ . Surface tension measurements were carried out using Kruss (Hamburg, Germany) Easy dyne tensiometer using ring detachment method at 298.15 K with an accuracy of  $\pm 0.15 \text{ mN m}^{-1}$ . Tensiometer was calibrated with double distilled water before measurements. The aqueous solution of SAILs were added into the aqueous polymer solution and stirred for two minutes to ensure proper mixing. The surface tension was measured after an equilibration time of 5 minutes. Conductivity was measured using a digital Systronics conductivity meter model 306 with a dip-type conductivity cell having a cell constant of  $1.01 \text{ cm}^{-1}$ . Temperature of the measurement cell was controlled using an Escy IC201 thermostatic bath within the accuracy of  $\pm 0.1$  K. Steady-state fluorescence measurements were performed using HITACHI F-1600 Fluorescence Spectrophotometer using a 10 mm path length quartz cuvette at 298.15 K employing pyrene as a fluorescent probe. Pyrene was excited at an excitation wavelength of 334 nm and emission spectrum was recorded in the wavelength range of 350-470 nm using an excitation and emission slit width of 2.5, each. To determine the aggregation numbers ( $N_{\text{agg}}$ ) of micelles in the absence and presence of polymer, cetyl pyridinium chloride

(CPC) was used as a quencher. Turbidity measurements were performed using Systronics Digital Nepheloturbidity Meter model 132 after equilibration for 5 minutes. Dynamic light scattering measurements were performed using a Malvern Zetasizer Nano-ZS instrument employing a He-Ne laser ( $\lambda = 632 \text{ nm}$ ) at 298.15 K at a scattering angle of  $173^\circ$ . The temperature of the measurement was maintained by built-in temperature controller having an accuracy of  $\pm 0.1 \text{ K}$ . The solutions were filtered through membrane filters ( $0.45 \mu\text{m}$ ) to remove dust particles. Calorimetric measurements were carried out using MicroCal ITC200 microcalorimeter. The titrations were done by adding  $2 \mu\text{L}$  aliquots of stock solutions of SAILs in  $240 \mu\text{L}$  of aqueous polymer solution using Hamilton syringe. All the measurements were carried out at 298.15 K and repeated twice. ITC measurements could only be performed for 10R5-[C<sub>10</sub>mim][Cl] and 10R5-[C<sub>12</sub>mim][Cl] mixed systems with high accuracy.

### 3. Results and discussion

#### 3.1. Tensiometric measurements

The interactional behavior of SAILs under investigation with block co-polymer, 10R5, at air-solution interface has been investigated using tensiometry. The variation of surface tension ( $\gamma$ ) as a function of concentration of SAILs in the absence and presence of  $0.5 \text{ mmol dm}^{-3}$  10R5 in aqueous solution for [C<sub>8</sub>mim][Cl], [C<sub>10</sub>mim][Cl], and [C<sub>12</sub>mim][Cl] is shown in Fig. 1 (a-c), respectively. The presence of polymer shows a marked decrease in  $\gamma$  of water from 72.8 to 48.4  $\text{mN m}^{-1}$  which indicates highly surface active nature of polymer. The tensiometric profiles of different SAILs have shown one minima before reaching a plateau indicating the onset of critical micelle concentration (*cmc*). The critical micelle concentrations of SAILs agree well their literature values [49, 50] and are given in Table 1. Various parameters of micellization of SAILs have been obtained from surface tension measurements and are provided in Table 1. Contrary to simple tensiometric profiles of SAILs, the outline of tensiometric profiles of SAILs in the presence of polymer, 10R5 show complicated behavior indicating the presence of interactions between SAILs and polymer. In all the investigated systems, three transitions in different concentration regimes, namely  $C_1$ ,  $C_2$  and  $C_3$ , designated as critical aggregation concentration (*cac*), critical saturation concentration of polymer ( $C_s$ ) and critical micelle concentration (*cmc*),

respectively, have been observed. The concentrations corresponding to these transitions are provided in Table 1. In dilute concentration regime,  $\gamma$  remains almost stable followed by a decrease at a concentration marked as  $C_1$  (*cac*). The *cac* indicates the onset of interactions between respective SAILs and polymer, 10R5 where the formation polymer-SAIL (monomer complex) at air-solution interface is expected. Beyond  $C_1$ ,  $\gamma$  decreases with a greater slope as a consequence of progressive formation of polymer-SAIL (aggregate) complex with increase in concentration of SAILs. The formation of polymer induced small micelles and their cooperative binding with the polymer sites at air-solution interface reduces  $\gamma$  up to a concentration marked as  $C_s$ . At  $C_s$ , all the binding sites available on polymer are saturated due to adsorption of SAIL on polymer backbone. With further addition of respective SAIL,  $\gamma$  decreases with a lower slope. This can be assigned to solubilization of some of the polymer-SAIL (aggregate) complex into bulk where at the same time, monomers of SAILs start populating the air-solution interface, thus reducing  $\gamma$  to  $C_3$  (*cmc*). At and above *cmc*, free micelles of SAILs are formed. At lower polymer concentration ( $0.5 \text{ mmol dm}^{-3}$ ) which is much below its *cmc*, the polymer molecules are present in monomeric form. It has been observed that at first, the PPO segments undergo dehydration from the water phase which is further followed by dehydration of PEO segments [16]. Therefore it is inferred that at first, the cationic component of SAIL bind to PEO segments and then to PPO segments through hydrophobic interactions. The phenomenon is described in Scheme 2. Our results showing three transitions are in contrast with those reported by Moulik *et al.*, [18] in which mixed micelle formation of reverse pluronic 10R5 and anionic surfactant sodium N-dodecanoylsarcosinate (SDDS) showed only two transitions i.e.  $C_s$  and *cmc*. The discrepancy is assigned to the difference in nature of surfactant head group where a positively charged head group of SAILs under investigation is assumed to interact with the 10R5 via hydrophobic as well as electrostatic and ion-dipole forces of interactions between lone pair of oxygen atom and the charged head group. Such interactions between ionic liquids (ILs) and water [49] have been reported. However, interactions of cationic gemini surfactants with triblock copolymers are somewhat more intricate than traditional ionic surfactants [8, 51]. Zheng *et al.*, [52] has reported that the surfactant head groups do not affect the intensity of interactions between surfactants and copolymers whereas increase in hydrophobicity of surfactant leads to increase in the interactions among them. On comparing the tensiometric profiles of all the three mixed

systems, it is clear that the *cac* depends on hydrophobicity of the chain length. This indicates that near to *cac*, SAIL monomers interact with 10R5 via hydrophobic interactions leading to formation of normal micellar structures on polymer backbone. The ratio of *cmc* to *cac* has been used to get insights into the affect of alkyl chain length of SAILs on their interactional behavior with polymer at air-solution interface. It has been observed that with increase in alkyl chain length, the ratio *cmc/cac* decrease which indicates that onset of formation of polymer induced micelles is delayed with increase in alkyl chain length. The main driving forces responsible for the interactions between 10R5 and SAILs in various concentration regimes seems to be hydrophobic and ion-dipole interactions in which hydrophobic interactions dominate in first concentration regime where aggregation of SAIL monomers start on the polymer backbone and later on, in higher concentration regions, ion-dipole forces also come into play.

Various thermodynamic parameters like surface tension at *cmc* ( $\gamma_{cmc}$ ), maximum surface excess concentration at the air-solution interface ( $\Gamma_{max}$ ), minimum area per molecule ( $A_{min}$ ), effectiveness of surface tension reduction ( $\pi_{cmc}$ ), Gibbs free energy of adsorption ( $\Delta G^{\circ}_{ads}$ ) (using  $\Delta G_{mic}$  from conductivity) have been calculated using the standard equations (Annexure S1, supporting information) and are given in Table 2. The values of  $\Gamma_{max}$  are minimum for [C<sub>8</sub>mim][Cl] as compared to other SAILs, in both aqueous and in polymer solution suggesting the relatively loose packing of [C<sub>8</sub>mim][Cl] at air-solution interface. The  $\Gamma_{max}$  values decrease in the presence of polymer in all the systems which commends that in the presence of the polymer, it is difficult for the SAILs to populate the air-solution interface effectively leading to formation of polymer-SAIL complexes. The  $A_{min}$  values decrease with the increase in alkyl chain length of SAILs in accordance with the literature reports [53] suggesting the increasing extent of packing of SAILs at air-solution interface with increase in alkyl chain length. Further, the values of  $A_{min}$  are more in the presence of polymer solution as compared to that in water which is in line with the variation of  $\Gamma_{max}$ . The  $\Delta G^{\circ}_{ads}$  values are more negative in water as compared to that in polymer solution indicating that the adsorption a air-solution interface is confined to some extent in the presence of polymer solution and is less feasible which is assigned to the surface active nature of polymer itself. Further the magnitude of  $\Delta G^{\circ}_{ads}$  don't vary much with variation in alkyl

chain length of SAIL in the presence of polymer confirming the higher affinity of the polymer at air-solution interface as compared to that for SAILs.

### 3.2. Conductivity measurements

The variation of conductivity as function of concentration of  $[C_{12}mim][Cl]$  in aqueous and aqueous solutions of polymer 10R5 in a temperature range 298.15 to 318.15 K is shown in Fig. 2(a-b) respectively, whereas respective plots for other SAILs are provided as supporting data (Fig. S1 a-d). The intersection of two linear fragments of different slopes in conductivity profiles indicates the *cmc*, after which, rate of increase in conductance become smaller because micelles have lower mobility than free ions and fraction of the counter ions are paired with the micelles. The ratio of slopes of post to pre-micellar region gives the degree of dissociation ( $\alpha$ ) which is further related to degree of counter ion binding ( $\beta$ ) by the equation  $\beta = 1 - \alpha$  [34]. The values of *cmc* and  $\beta$  of SAILs in aqueous and aqueous polymer solutions are given in Table 4 and 5. The *cmc* values of SAILs have been found to be in good agreement with those obtained from surface tension measurements and with literature at 298.15 K [49, 50]. The *cmc* values of SAILs increases in presence of polymer as SAILs saturate the polymer surface before undergoing micellization, leading to delay in micellization process. An increase in temperature has also been found to retard the micellization. This can be ascribed to the aspect that the increase in temperature increases the solubility of hydrophobic chains which disrupt the iceberg structure surrounding the hydrophobic chain and thus, it delays the micelle formation [54]. However, it is well established that with increase in temperature, the PPO and PEO blocks undergo dehydration, which is also expected to have a role in delaying of *cmc*. It is clear from the values given in the Table 5 that  $\beta$  increases with the increase in alkyl chain length of SAIL and is maximum for  $[C_{12}mim][Cl]$  in both aqueous and aqueous polymer solution. This indicates that with the increase in chain length, more compact micelles are formed and counter ions are firmly bound to the stern layer. On comparing the  $\beta$  values of SAILs in aqueous and in aqueous polymer solution, it has been observed that  $\beta$  values are relatively small in the presence of polymer. This can be explained on the assumption that just before micellization or upon micellization, the polymer segments undergo rehydration and bound to the outer region of

micelles via hydrophobic and electrostatic interactions, leading to stabilization of micelles resulting in decrease in  $\beta$  to some extent as that of aqueous solution.

The Gibbs free energy of micelle formation,  $\Delta G_{mic}$  was calculated using the equation [34] (1):

$$\Delta G_{mic} = (1 + \beta)RT \ln X_{cmc} \quad (1)$$

Where, R, T and  $X_{cmc}$  are gas constant, temperature on Kelvin scale and  $cmc$  expressed in mole fraction. The enthalpy of micelle formation,  $\Delta H_{mic}$  was calculated by employing Gibbs-Helmholtz equation using free energy of micellization.

$$\Delta H_{mic} = \frac{-T^2 \partial(\Delta G_{mic}/T)}{\partial T} \quad (2)$$

Then the entropy of micelle formation,  $\Delta S_{mic}$  is obtained as:

$$\Delta S_{mic} = \frac{\Delta H_{mic} - \Delta G_{mic}}{T} \quad (3)$$

The thermodynamic parameters obtained are given in Table 4 and 5. The negative values of  $\Delta G_{mic}$  suggest that micellization process is spontaneous. The  $\Delta G_{mic}$  values become more negative with the increase in alkyl chain length of SAIL as expected. However,  $\Delta G_{mic}$  become less negative in the presence of polymer for all investigated polymer-SAIL mixed systems as compared to that in the absence of polymer. As can be seen from Table 4 and 5, the negative values of  $\Delta G_{mic}$  are contributed by negative values of  $\Delta H_{mic}$  over the whole temperature range, similar to that observed in case of aqueous solutions. It has been observed that hydrophobic effect and electrostatic interactions are mainly responsible for micellization in aqueous media [55] and the micellization process is an enthalpy-driven phenomenon. However in case of  $[C_{12}mim][Cl]$ , the entropy factor contributes significantly towards free energy change relative to that in other systems in the presence of polymer.

### 3.3. Calorimetric measurements

Isothermal titration calorimetry (ITC) is a versatile technique for acquiring information regarding self-organization of surfactants into micelles which permits the determination of critical micelle concentration ( $cmc$ ) and the enthalpy of micellization ( $\Delta H$ ) in a single experiment without the need of any probe [56-58]. The enthalpograms of SAILs,  $[C_{10}mim][Cl]$  and  $[C_{12}mim][Cl]$  in the presence and absence of  $0.5 \text{ mmol dm}^{-3}$  10R5 aqueous polymer as a function of concentration of SAILs are shown in Fig. 3(a-b), respectively, and the corresponding profiles for differential enthalpy ( $dP$ ) for SAILs in aqueous and polymer solution are shown in Fig. S3 and Fig. S4 respectively (supporting information). For  $[C_8mim][Cl]$ , a very high concentration of SAIL is required ( $3 \text{ mol dm}^{-3}$ ) and even with such high concentration, micellization process is not complete. Due to this,  $cmc$  and  $\Delta H_{mic}$  for this SAIL could not be obtained using ITC measurements. The shape of the enthalpograms obtained can be rationalized in terms of polymer induced formation of aggregates of SAIL on or near the hydrophobic sites of polymer [59]. From Fig. 3(a-b), it is obvious that the enthalpograms obtained for aqueous solution of SAILs in the presence of 10R5 are different from that obtained in absence of polymer at least in the magnitude, which is a direct consequence of the interaction between the two components. Inset of Fig. 3(a-b) shows the differential thermogram, which has been obtained by subtracting the enthalpograms obtained in the absence of  $0.5 \text{ mmol dm}^{-3}$  of 10R5 from that obtained in the presence of  $0.5 \text{ mmol dm}^{-3}$  of 10R5 to get a concise view of the events. As can be seen from inset of Fig. 3(a) and (b), for the system having  $[C_{10}mim][Cl]$ , two transitions namely,  $C_2$  and  $C_3$  have been observed, whereas in case of system having  $[C_{12}mim][Cl]$ , three transitions namely  $C_1$ ,  $C_2$  and  $C_3$  have been observed. The obtained values of different transitions are tabulated in Table 3. The heat changes involved are mainly due to dissociation of micelles into monomers before  $cmc$ , dilution effects, dehydration or rehydration of polymer segments and binding interactions between surfactant in monomeric form and in micellar form (after  $cmc$ ) with polymer. For 10R5- $[C_{10}mim][Cl]$  systems, the titration curve has been found to be sigmoidal in shape. In the first few injections of  $[C_{10}mim][Cl]$  ( $C \leq 13.0 \text{ mmol dm}^{-3}$ ), endothermic heat changes occur which is due to demicellization of concentrated solution of  $[C_{10}mim][Cl]$  and is likely to be affected by dehydration of PPO/PEO segments where the monomers of  $[C_{10}mim][Cl]$  bind to the polymer through hydrophobic interactions leading to formation of polymer-SAIL (monomer) complexes in this concentration regime. With the increase in concentration of

respective SAIL ( $13.0 \text{ mmol dm}^{-3} < C > cmc$ ), the magnitude of endothermic change increase to reach a maximum and gives the critical saturation concentration ( $C_s$ ) where polymer-SAIL (aggregate) complex are formed. The  $C_s$  value obtained from calorimetry is higher than those obtained from techniques discussed earlier. This might be due to fact that different techniques sense different stages of interactions. After  $C_s$ , the concentration of unbound monomers exceeds the  $cmc$ , and here occurs the onset of micellization where the added micelles no longer dissociate into monomers that lead to decrease in enthalpy. As also indicated by other techniques, it is anticipated that the PEO segments undergo rehydration in this concentration regime and bind to the surface of micelles via ion-dipole interactions and resulting in exothermic heat changes.

For 10R5- $[C_{12}mim][Cl]$  system, at low concentration of  $[C_{12}mim][Cl]$  ( $C \leq 3.0 \text{ mmol dm}^{-3}$ ), the added micelles dissociate into monomers which bind to polymer that results in formation of polymer-SAIL (monomer) complex and thus, endothermic heat changes take place. In higher concentration regime *i.e.*  $3.0 \text{ mmol dm}^{-3} < C > cmc$ , polymer gets saturated with the SAIL monomers and gives the critical saturation concentration ( $C_s$ ). With further addition of  $[C_{12}mim][Cl]$ , free micelles of SAIL start forming at and above  $cmc$ . The values of various transitions for 10R5- $[C_{12}mim][Cl]$  are in well agreement with those obtained from other techniques. The thermodynamic parameter *i.e.* Gibbs free energy, ( $\Delta G_{mic}$ ) of interaction between 10R5 and SAILs has been calculated using the  $cmc$  obtained from ITC and degree of counter-ion binding ( $\beta$ ) obtained from conductivity measurements [18]. The corresponding value of entropy change ( $\Delta S$ ) is calculated using the Gibbs-Helmholtz equation.

The calculated values of different thermodynamic parameters ( $\Delta H$ ,  $\Delta G$ ,  $\Delta S$ ) corresponding to different transitions observed from ITC are shown in Table 3. A keen analysis of Table 3 reveals that enthalpy changes are exothermic as well as endothermic for various transitions in polymer-SAIL mixed systems. The enthalpy changes ( $\Delta H$ ) corresponding to  $cmc$  and  $C_s$  are endothermic and whereas they are exothermic for  $cmc$  and listed in Table 3. At sufficiently high concentration of both the SAILs, the dilution curves are near to merge with those obtained in water. The obtained  $\Delta G_{mic}$  at  $cmc$  is in good agreement with that obtained from conductivity measurements at 298.15 K. However, there are differences in values of other

thermodynamic parameters. The differences arise due to various physicochemical processes other than aggregation responsible for heat changes. Calorimetry involves integral heat of process whereas conductivity gives differential heat of micellization. Also, counterion binding of aggregates and dynamic nature of aggregation strongly influence  $\Delta H_{\text{mic}}$  values in calorimetry but these factors do not have pronounced effect in conductivity measurements [60].

### 3.4. Turbidity measurements

The plots for variation in turbidity in 10R5-[C<sub>8</sub>mim][Cl], -[C<sub>10</sub>mim][Cl], and -[C<sub>12</sub>mim][Cl] systems are shown in Fig. 4(a-c), respectively. For all the investigated systems, turbidity initially increases slightly with the increase in concentration of SAILs up to  $C_1$  (observed in surface tension). Above  $C_1$ , turbidity increases sharply up to a concentration  $C_s$  which is due to formation of polymer-SAIL (aggregate) complex at  $C_s$ . The increase in size of the forming polymer-SAIL (aggregate) complex with an increase in concentration of SAIL leading to increase in turbidity also cannot be ruled out. Above  $C_s$ , turbidity increases with a slightly lower slope and reaches a maximum at  $C_3$  (*cmc*). This increase in turbidity is due to phase separation behavior by virtue of hydrophobic interactions between PPO segments of polymer and alkyl chain of SAIL in polymer-SAIL (aggregate) complex. The behavior of turbidity changes is different from that reported by Singh et al. [41] between gelatin-[C<sub>8</sub>mimCl] mixed systems in which only two transitions have been observed as the nature of polymer used and charge on the polymer affects their interaction with surfactants. Above *cmc*, the turbidity decreases initially followed by a constant value in case of 10R5-[C<sub>10</sub>mim][Cl] and 10R5-[C<sub>12</sub>mim][Cl]. The decrease in turbidity after *cmc* indicates the partial solubilization of polymer-SAIL (aggregate) complex by the formed micelle which remains stable in the presence of micelles. However in 10R5-[C<sub>8</sub>mim][Cl], no such phenomenon of solubilization of polymer-SAIL (aggregate) complex has been observed as indicated by constant turbidity after *cmc*.

### 3.5. Fluorescence measurements.

Fluorescence of pyrene is highly sensitive to polarity of the medium and the ratio of first and third vibronic peak ( $I_1/I_3$ ) is used as a measure of polarity [61]. The ratio of  $I_1/I_3$  decreases with

the decrease in polarity of the medium. Fig. 5 (a-c) represents the variation of  $I_1/I_3$  as a function of concentration of  $[C_8mim][Cl]$ ,  $[C_{10}mim][Cl]$ , and  $[C_{12}mim][Cl]$ , respectively, in water and in aqueous polymer solutions. For all the investigated systems,  $I_1/I_3$  shows a constancy initially up to a concentration corresponding to  $C_s$  followed by a sharp decrease until it reaches a plateau at  $cmc$ . No transition corresponding to  $C_1$  ( $cac$ ) has been observed from fluorescence measurements indicating the non-formation of any hydrophobic domains in polymer-SAIL (monomer) complex at the sensing level of pyrene. At  $C_s$ , the polymer backbone is saturated with the monomers of SAILs, and a decrease in  $I_1/I_3$  beyond  $C_s$  is due to the formation of polymer-SAIL (aggregate) complex which exhibit decreased hydrophilic character. The  $cmc$  values obtained from fluorescence are smaller than those obtained from surface tension and are in lines with conductometry as different techniques senses different techniques of micellization. The  $I_1/I_3$  values at  $cmc$  for the 10R5- $[C_8mim][Cl]$ ,  $[C_{10}mim][Cl]$ ,  $[C_{12}mim][Cl]$  systems are 1.54, 1.41, 1.31 indicating an increase in hydrophobic character of micelle with increase in alkyl chain length of SAIL. Very interestingly, the  $I_1/I_3$  values in the presence of polymer have found to be higher as compared to that observed in the absence of polymer. This indicates that the pyrene occupies relatively less hydrophobic region in the presence of polymer most probably in the polymer-SAIL (aggregate) complex along with the free micelles and an average of the environment of pyrene has been detected. Further, the presence of water in vicinity of polymer-SAIL (aggregate) complex leading to relatively higher value to  $I_1/I_3$  cannot be ruled out.

The aggregation number ( $N_{agg}$ ) is a characteristic feature of surfactants which gives the average number of surfactants forming the micelle. The  $N_{agg}$  of investigated SAILs in aqueous and in aqueous polymer solution has been determined by steady-state fluorescence quenching technique using the method described by Turro-Yekta [62] employing pyrene and CPC as fluorescent probe and quencher, respectively, using the relation:

$$\ln\left(\frac{I_0}{I}\right) = \frac{N_{agg}[Q]}{[S]_T - cmc} \quad (4)$$

Where,  $I_0$  and  $I$  are the fluorescence intensities in the absence and presence of quencher, respectively,  $[Q]$  is concentration of quencher,  $S_T$  gives the total concentration of surfactant. Fig.

S2(a-b) (supporting information) shows the variation of  $\ln(I_0/I)$  versus  $[Q]$ , the slope of which have been used to calculate the  $N_{agg}$  for SAILs in absence and presence of polymer. The  $N_{agg}$  of SAILs in the absence and presence of polymer are given in Table 2. The  $N_{agg}$  of the SAILs  $[C_8mim][Cl]$ ,  $[C_{10}mim][Cl]$ ,  $[C_{12}mim][Cl]$  in aqueous solution are 40, 45, 56 and found to be in good agreement with their literature values [63, 64]. The  $N_{agg}$  of SAILs decreases in the presence of polymer which is a normal behavior observed for surfactants-polymer systems [65] as the presence of polymer restricts the formation of large aggregates which is liable for the decrease in  $N_{agg}$  in polymer solution.

### 3.6. Morphology of polymer-SAIL aggregates

Dynamic light scattering studies have been carried out to investigate the changes in hydrodynamic diameter,  $D_h$  of the complexes formed between polymer and SAIL in different concentration regime of respective SAILs. The variation of  $D_h$  for aqueous polymer systems ( $0.5 \text{ mmol dm}^{-3}$ ) as a function of concentration for  $[C_8mim][Cl]$ ,  $[C_{10}mim][Cl]$ , and  $[C_{12}mim][Cl]$  are presented in Fig. 6(a-c), respectively. The values of  $D_h$  along with poly dispersity index (*PDI*) as a function of concentration of respective SAIL in mixed systems is provided in Table S1 (supporting information). The schematic representation showing the binding interaction mechanism between 10R5 and SAILs adopted based on the observations made from various techniques is shown as scheme 2. The  $D_h$  of native  $0.5 \text{ mmol dm}^{-3}$  10R5 is  $\approx 3.1 \text{ nm}$  indicating the presence of polymer as random coil in water at this concentration. In the case of 10R5- $[C_{12}mim][Cl]$ , upon the addition of  $[C_{12}mim][Cl]$ ,  $D_h$  size increases initially up to a concentration of  $7.0 \text{ mmol dm}^{-3}$  to  $D_h$  of 90 nm, which further shows a rapid decrease to a size of 12 nm at a concentration of  $9.1 \text{ mmol dm}^{-3}$ . The initial increase in  $D_h$  is due to interaction between polymer and monomers of  $[C_{12}mim][Cl]$  which result in formation of expanded polymer-SAIL (monomer) complex as shown scheme 2 (step-I to III). Such large increase in size of aggregates from 3 to 90 nm can be due to counter-ion mediated electrostatic interactions between charged species [66]. Therefore, It is assumed that a few polymer-SAIL (monomer) complexes comes together intermediated by counter-ions to form large sized aggregates as shown in Scheme 2. This concentration range falls between  $C_s$  and *cmc* values obtained from

surface tension plots. On further addition of  $[C_{12}mim][Cl]$ , size increases only slightly and remains constant afterwards. The concentration corresponding to endothermic maximum appearing in ITC thermogram (Fig. 5b) also matches well with the concentration of maximum  $D_h$  which reveals that monomers of SAIL are absorbed on the PPO block through hydrophobic interactions and thus, they form large mixed aggregates with the polymer corroborating well with DLS data. Further, increase in concentration of SAIL induces electrostatic repulsions between similarly charged head groups and thus destabilizes the micelles resulting in the decrease in size of the polymer-SAIL complexes and the consequence is the formation of smaller mixed micelles of polymer and  $[C_{12}mim][Cl]$ . In case of 10R5- $[C_{10}mim][Cl]$ , on small addition of SAIL, size increases abruptly to a size of 77 nm around a concentration of  $2.0 \text{ mmol dm}^{-3}$  which matches with  $C_1$  as obtained from surface tension and turbidity measurements. The size further increases to a maximum size of 122 nm with further addition of SAIL up to  $26 \text{ mmol dm}^{-3}$ , which is followed by a decrease up to a concentration of  $35.6 \text{ mmol dm}^{-3}$  which corresponds to *cmc* of SAIL, which is also evidenced from other techniques employed. The size further remains constant on the addition of SAIL in corroboration with the turbidity measurements. In case of 10R5- $[C_8mim][Cl]$ ,  $D_h$  remains constant upto  $8.4 \text{ mmol dm}^{-3}$  which suggests that short chain  $[C_8mim][Cl]$  adsorbs relatively to lesser extent onto the polymeric backbone initially as compared to other SAILs possibly due to decreased hydrophobic interactions and then increases to attain a plateau around  $C_2$ . The appearance of plateau in the mixed systems indicates the saturation of polymer backbone due to adhered aggregates of SAIL. This is followed by a decrease in size at  $131.0 \text{ mmol dm}^{-3}$ . The size further increases with the increase in concentration which indicates that free micelles of SAIL are formed which are growing in size.

#### 4. Conclusions

The present work is focused on the interactions between triblock reverse copolymer 10R5 and surface active ionic liquids (SAILs),  $[C_8mim][Cl]$ ,  $[C_{10}mim][Cl]$ , and  $[C_{12}mim][Cl]$  using multi-technique approach. The interactions between 10R5 and SAILs are illustrated in terms of different concentration regimes and these interactions are mainly driven by ion-dipole among cationic head group of SAILs with PEO blocks and hydrophobic interactions between

hydrophobic chain length of SAILs and PPO blocks of 10R5. The ratio of these interactional modes in the described concentration regions is different. The various techniques employed give the same picture of interactions between 10R5 and SAILs. Tensiometry has revealed that in very dilute concentration regime of SAIL *i.e.* at *cac*, polymer-SAIL (monomer) complex is formed on the polymer backbone which later transformed to polymer-SAIL (aggregates) complex at higher concentration of SAIL. The calculated thermodynamic parameters using conductivity and isothermal titration calorimetry techniques suggest that the micellization process in the presence of polymer is an enthalpy driven in investigated temperature range where maximal entropic contribution has been observed in case of [C<sub>12</sub>mim][Cl]. Thermodynamic analysis reveals that hydrophobic interactions play an important role in mixed micellization of proposed systems. Fluorescence measurements have suggested that the hydrophobicity of the formed complexes between polymer and SAILs increases with increase in alkyl chain length of SAIL. The turbidity and dynamic light scattering measurements also indicate the presence the three concentration regions and the results obtained are in corroboration with those extracted from other techniques. In nut shell, we conclude that micellization of polymer and SAILs are governed by hydrophobic interactions as well as ion-dipole interactions and these interactions increase with the increase in alkyl chain length of SAILs. The polymer-SAILs mixed systems have tremendous potential which can be utilized in future in many fields to get more economical, environment friendly mixed systems with improved characteristics like viscosity, surface activity and solubilization.

### **Acknowledgement**

This work was financially supported by the Department of Science and Technology (DST) New Delhi, India as a part of Project NO.SR/S1/PC-02/2011. Renu Sharma is thankful to University Potential for Excellence (UPE) scheme, Guru Nanak Dev University, Amritsar for the award of research fellowship (RF).

## References

1. V.P. Torchilin, *J. Controlled Rel.* 73 (2001) 137-172.
2. T. Moore, C. Scott, M. Surya. P. Nivedita, *J. Controlled Rel.* 67 (2000) 191-202.
3. A. Lavasanifar, J. Samuel, G.S. Kwon, *Adv. Drug Delivery Rev.* 54 (2002) 169-190.
4. Z. Zhou, B. Chu, *Macromolecules* 27 (1994) 2025-2033.
5. J.S. Namban, J. Philip, *J. Phys. Chem. B* 116 (2012) 1499-1507.
6. C. Wu, T. Liu, B. Chu, D.K. Schneider, V. Graziano, *Macromolecules* 30 (1997) 4574-4583.
7. J.B. Vieira, R.K. Thomas, Z.X. Li, J. Penfold, *Langmuir* 21 (2005) 4441-4451.
8. X. Li, S.D. Wettig, R.E. Verall, *J. Colloid Interface Sci.* 282 (2005) 466-477.
9. K.S. Mali, G.B. Dutt, T. Mukherjee, *J. Phys. Chem. B* 111 (2007) 5878-5884.
10. R. Ganguly, V.K. Aswal, P.A. Hassan, I.K. Gopalakrishnan, J.V. Yakhmi, *J. Phys. Chem. B* 109 (2005) 5653-5658.
11. R. Kaur, S. Kumar, V.K. Aswal, R.K. Mahajan, *Langmuir* 29 (2013) 11821-11833.
12. R. Sanan, R.K. Mahajan, *Colloids Surf. A* 433 (2013) 145-153.
13. R. Sharma, A. Shaheen, R.K. Mahajan, *Colloid Polym. Sci.* 289 (2011) 43-51.
14. O. Ortona, G.D. Errico, L. Paduano, V. Vitagliano, *J. Colloid Interface Sci.* 301 (2001) 63-77.
15. J. Mata, T. Joshi, D. Varade, G. Ghosh, P. Bahadur, *Colloids Surf. A* 247 (2004) 1-7.
16. S. Dai, K.C. Tam, L. Li, *Macromolecules* 34 (2001) 7049-7055.
17. B. Naskar, S. Ghosh, S.P. Moulik, *J. Colloid Interface Sci.* 414 (2014) 82-89.
18. B. Naskar, S. Ghosh, S.P. Moulik, *Langmuir* 28 (2012) 7134-7146.
19. T. Welton, *Chem. Rev.* 99 (1999) 2071-2084.
20. J.L. Anderson, V. Pino, E.C. Hagberg, V.V. Sheares, D.W. Armstrong, *Chem. Commun. (Cambridge)* 19 (2003) 2444-2445.
21. P.T.P. Thi, C.W. Cho, Y.S. Yun, *Water Res.* 44 (2010) 352-372.
22. R.D. Rogers, K.R. Seddon, *Science* 302 (2003) 792-793.
23. P. Kubisa, *Prog. Polym. Sci.* 29 (2004) 3-12.

24. J.M. Crosthwaite, M.J. Muldoon, J.K. Dixon, J.L. Anderson, J.F. Brennecke, *J. Chem. Thermodyn.* 37 (2005) 559-568.
25. A.E. Jimenez, M.D. Bermudez, *Tribol. Lett.* 26 (2007) 53-60.
26. C.P. Mehnert, R.A. Cook, N.C. Dispenziere, M. Afeworki, *J. Am. Chem. Soc.* 124 (2002) 12932-12933.
27. A.B. Mcewen, H.L. Ngo, K. Lecompte, J.L. Goldman, *J. Electrochem. Soc.* 146 (1999) 1687-1695.
28. K. Ding, Z. Miao, Z. Liu, G. An, Y. Xie, R. Tao, B. Han, *J. Mater. Chem.* 18 (2008) 5406-5411.
29. H. Kaper, S. Sallard, I. Djerdj, M. Antonietti, B.M. Smarsly, *Chem. Mater.* 22 (2010) 3502-3510.
30. Q. Ji, S. Acharya, G.J. Richards, S. Zhang, J. Vieaud, J.P. Hill, K. Ariga, *Langmuir* 29 (2013) 7186-7194.
31. R. Sharma, R.K. Mahajan, *RSC Adv.* 4 (2014) 748-774.
32. J. Luczak, J. Hupka, J. Thoming, C. Jungnickel, *Colloids Surf. A*, 329 (2008) 125-133.
33. S. Mahajan, R. Sharma, R.K. Mahajan, *Langmuir* 28 (2012) 17238-17246.
34. R. Sanan, T.S. Kang, R.K. Mahajan, *Phys. Chem. Chem. Phys.* 16 (2014) 5667-5677.
35. T. Singh, A. Kumar, *J. Phys. Chem. B* 111 (2007) 7843-7851.
36. G. Bai, A. Lopes, M. Bastos, *J. Chem. Thermodyn.* 40 (2008) 1509-1516.
37. M. Blesic, M.H. Marques, N.V. Plechkova, K.R. Seddon, L.P.N. Rebelo, A. Lopes, *Green Chem.* 9 (2007) 481-490.
38. J. Wang, H. Wang, S. Zhang, H. Zhang, Y. Zhao, *J. Phys. Chem. B* 111 (2007) 6181-6188.
39. T.J. Trivedi, K.S. Rao, T. Singh, S.K. Mandal, N. Sutradhar, A.B. Panda, A. Kumar, Task-specific, biodegradable amino acid ionic liquid surfactants, *ChemSusChem* 4 (2011) 604-608.
40. B. Dong, N. Li, L. Zheng, L. Yu, T. Inoue, Surface formation and micelle formation of surface active ionic liquid in aqueous solution, *Langmuir* 23 (2007) 4178-4182.
41. T. Singh, S. Boral, H.B. Bohidar, A. Kumar, Interaction of gelatin with room temperature ionic liquids: A detailed physicochemical study, *J. Phys. Chem. B* 114 (2010) 8441-8448.

42. P. Bharmoria, A. Kumar, RSC Adv. 3 (2013) 19600-19608.
43. P. Bharmoria, T. Singh, A. Kumar, J. Colloid Interface Sci. 407 (2013) 361-369.
44. X. Wang, J. Liu, L. Sun, L. Yu, J. Jiao, R. Wang, J. Phys. Chem. B 116 (2012) 12479-12488.
45. T. Singh, P. Bharmoria, M. Morikawa, N. Kimizuka, A. Kumar, J. Phys. Chem. B 116 (2012) 11924-11935.
46. L. Zheng, C. Guo, J. Wang, X. Liang, S. Chen, J. Ma, B. Yang, Y. Jiang, H. Liu, J. Phys. Chem. B 111 (2007) 1327-1333.
47. T. Inoue, H. Yamakawa, J. Colloid Interface Sci. 356 (2011) 798-802.
48. P.M. Reddy, P. Venkatesu, J. Colloid Interface Sci. 420 (2014) 166-173.
49. C. Jungnickel, J. Luczak, J. Ranke, J.F. Fernandez, A. Muller, J. Thoming, Colloids Surf. A 316 (2008) 278-284.
50. P.D. Galeno, O.A. El Seoud, J. Colloid Interface Sci. 361 (2011) 186-194.
51. R. Wang, Y. Tang, Y. Wang, Langmuir 30 (2014) 1957-1968.
52. J. Liu, M. Zhao, Q. Zhang, D. Sun, X. Wei, L. Zheng, Colloid Polym. Sci. 289 (2011) 1711-1718.
53. B. Dong, X.Y. Zhao, L.Q. Zheng, J. Zhang, N. Li, T. Inoue, Colloids Surf. A 317 (2008) 666-672.
54. Y. Wei, F. Wang, Z. Zhang, C. Ren, Y. Lin, J. Chem. Eng. Data 59 (2014) 1120-1129.
55. D. Myers, Surfaces, Interfaces and Colloids: Principles and Applications: 2<sup>nd</sup> Ed., Wiley-VCH: New York, 1999.
56. N.M. Vas Os, G.J. Daane, G. Haandrikman, J. Colloid Interface Sci. 141 (1991) 199-217.
57. B. Anderson, G. Olofsson, J. Chem. Soc. Faraday Trans. 1 (1988) 4087-4095.
58. G. Olofsson, G. Wang, in: J.C.T. Kwak (Ed.), Polymer-Surfactant Systems, Surfactant Science Series, 77, Marcel Dekker, New York, 1998 pp. 318-356.
59. G. Wang, G. Olofsson, J. Phys. Chem. B 102 (1998) 9276-9283.
60. A. Chatterjee, S.P. Moulik, S.K. Sanyal, B.K. Mishra, P.M. Puri, J. Phys. Chem. B 105 (2001) 12823-12831.
61. K. Kalyanasundaram, J.K. Thomas, J. Am. Chem. Soc. 99 (1977) 2039-2044.
62. N.J. Turro, A. Yekta, J. Am. Chem. Soc. 100 (1978) 5951-5952.

63. N.M. Vaghele, N.V. Sastry, V.K. Aswal, *Colloid Polym. Sci.* 289 (2011) 309-322.
64. O.A. El Seoud, P.A.R. Pires, T. Abdel-Moghny, E.L. Bastos, *J. Colloid Interface Sci.* 313 (2007) 296-304.
65. O. Ortona, G. D'Errico, L. Paduano, R. Sartorio, *Phys. Chem. Chem. Phys.* 4 (2002) 2604-2611.
66. S. Perkin, *Phys. Chem. Chem. Phys.* 14 (2012) 5052-5062.

### Figure Captions

Scheme 1. Molecular Structures of (a) 1-alkyl-3-methyl imidazolium chloride (SAIL) (b) Reverse pluronic 10R5.

Scheme 2. Schematic presentation of binding interactions between polymer 10R5 and surface active ionic liquids (SAILs).

Fig. 1. Variation of surface tension ( $\gamma$ ) as a function of logarithm of concentration of SAIL (a)  $[C_8mim][Cl]$ ; (b)  $[C_{10}mim][Cl]$ ; and (c)  $[C_{12}mim][Cl]$ .

Fig. 2. Variation of specific conductivity ( $\kappa$ ) as a function of concentration of  $[C_{12}mim][Cl]$  in the (a) absence; and (b) presence of polymer 10R5 at different temperatures.

Fig. 3. Calorimetric profiles of SAILs as a function of concentration (a)  $[C_{10}mim][Cl]$ ; and (b)  $[C_{12}mim][Cl]$  in the absence and presence of polymer 10R5 (Inset shows the differential thermogram obtained in the presence and absence of polymer 10R5).

Fig. 4. Variation of turbidity versus concentration of SAILs in polymer solution (a)  $[C_8mim][Cl]$ ; (b)  $[C_{10}mim][Cl]$ ; and (c)  $[C_{12}mim][Cl]$ .

Fig. 5. Variation of  $I_1/I_3$  versus concentration of SAILs (a)  $[C_8mim][Cl]$ ; (b)  $[C_{10}mim][Cl]$ ; and (c)  $[C_{12}mim][Cl]$ .

Fig. 6. Variation of hydrodynamic diameter ( $D_h$ ) versus concentration of SAILs in the aqueous solution of polymer, 10R5 (a)  $[C_8mim][Cl]$ ; (b)  $[C_{10}mim][Cl]$ ; and (c)  $[C_{12}mim][Cl]$ .

Table 1. Interaction characteristic concentrations ( $\text{mmol dm}^{-3}$ ) observed from surface tension (S.T.), fluorescence (Flu.), turbidity (Turb.) and conductance (Cond.) measurements in the absence and presence of polymer 10R5 at 298.15K.

	S.T.	Flu.	Turb.	Cond.
<i>cmc</i>	168.4(234) <sup>a</sup>	Pure [C <sub>8</sub> mim][Cl]	172.0	158.4(220) <sup>a</sup>
		152.5		
		10R5-[C <sub>8</sub> mim][Cl]		
<i>C</i> <sub>1</sub> ( <i>cac</i> )	7.4	-	17.6	-
<i>C</i> <sub>2</sub> ( <i>C</i> <sub>s</sub> )	50.4	74.2	68.4	-
<i>C</i> <sub>3</sub> ( <i>cmc</i> )	190.5	172.2	180.0	158.6
<i>cmc</i>	35.3(53.8) <sup>a</sup>	Pure [C <sub>10</sub> mim][Cl]	30.1	39.8(56.4) <sup>b</sup>
		32.6		
		10R5-[C <sub>10</sub> mim][Cl]		
<i>C</i> <sub>1</sub> ( <i>cac</i> )	2.1	-	3.5	-
<i>C</i> <sub>2</sub> ( <i>C</i> <sub>s</sub> )	8.1	8.4	16.7	-
<i>C</i> <sub>3</sub> ( <i>cmc</i> )	36.6	35.8	37.7	40.4
<i>cmc</i>	12.3	Pure [C <sub>12</sub> mim][Cl]	16.4	14.9(14.1) <sup>b</sup>
		14.1		
		10R5-[C <sub>12</sub> mim][Cl]		
<i>C</i> <sub>1</sub> ( <i>cac</i> )	2.0	-	2.4	-
<i>C</i> <sub>2</sub> ( <i>C</i> <sub>s</sub> )	4.8	5.2	10.0	-
<i>C</i> <sub>3</sub> ( <i>cmc</i> )	16.4	13.8	17.0	16.4

<sup>a,b</sup> refer to ref.49,50

Table 2. Interfacial parameters *i.e.* surface tension at *cmc* ( $\gamma_{cmc}$ ), effective surface tension reduction ( $\Pi_{cmc}$ ), surface excess ( $\Gamma_{max}$ ), minimum area per molecule ( $A_{min}$ ), Gibbs free energy of adsorption ( $\Delta G^{\circ}_{ads}$ ) and aggregation number ( $N_{agg}$ ) of SAILs in the absence and presence of polymer 10R5 at 298.15K.

	$\gamma_{cmc}$ (mN m <sup>-1</sup> )	$\pi_{cmc}$ (mN m <sup>-1</sup> )	$\Gamma_{max} \times 10^6$ (mol dm <sup>-3</sup> )	$A_{min}$ (Å <sup>2</sup> )	$\Delta G^{\circ}_{ads}$ kJ mol <sup>-1</sup>	$N_{agg}$
SAILs in water						
[C <sub>8</sub> mim][Cl]	32.4	38.8	1.6	103.0	-42.9	40
[C <sub>10</sub> mim][Cl]	26.4	44.9	2.1	80.0	-45.6	45
[C <sub>12</sub> mim][Cl]	31.2	40.0	2.3	71.4	-48.8	56
SAILs in 0.5mmol dm <sup>-3</sup> 10R5						
[C <sub>8</sub> mim][Cl]	31.7	16.7	0.7	233.6	-42.1	25
[C <sub>10</sub> mim][Cl]	27.6	20.8	1.1	144.9	-42.7	35
[C <sub>12</sub> mim][Cl]	32.1	16.3	1.3	131.8	-42.6	38

Table 3. Critical micelle concentration, Gibbs free energy ( $\Delta G_{mic}$ ), enthalpy ( $\Delta H_{mic}$ ) and entropy ( $\Delta S_{mic}$ ) of micellization of SAILs in the presence of polymer 10R5 as obtained from isothermal titration calorimetry studies at 298.15 K.

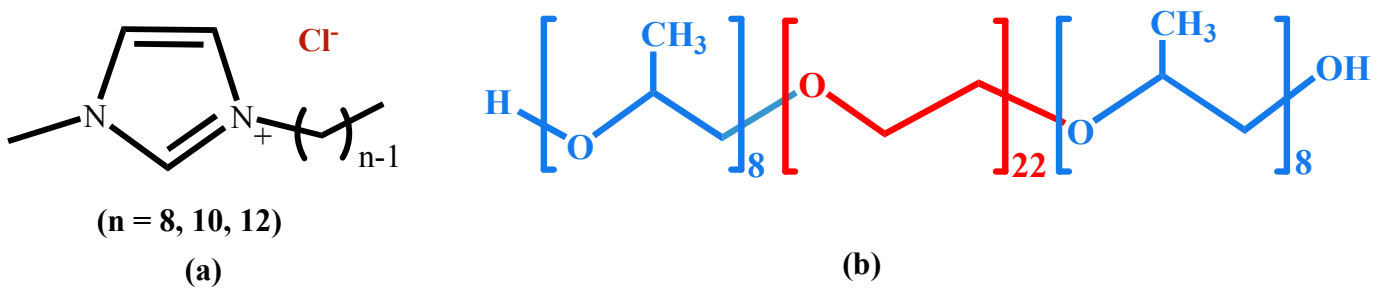
In 0.5 mmol dm <sup>-3</sup> 10R5	$cac/C_s/cmc$ mmol dm <sup>-3</sup>	$\Delta G_{cac}/\Delta G_{C_s}/\Delta G_{cmc}$ kJ mol <sup>-1</sup>	$\Delta H_{cac}/\Delta H_{C_s}/\Delta H_{cmc}$ kJ mol <sup>-1</sup>	$\Delta S_{cac}/\Delta S_{C_s}/\Delta S_{cmc}$ JK <sup>-1</sup> mol <sup>-1</sup>
[C <sub>10</sub> mim][Cl]	-/25.4/36.6	-/-25.5/-24.3	-/-3.7/-0.8	-/73.3/84.1
[C <sub>12</sub> mim][Cl]	2.5/7.5/13.3	-36.7/-32.7/-30.6	0.8/4.6/-5.3	125.8/124.9/84.7

Table 4. Critical micelle concentration ( $cmc$ ), degree of counter ion binding ( $\beta$ ), Gibbs free energy of micellization ( $\Delta G_{mic}$ ), enthalpy of micellization ( $\Delta H_{mic}$ ) and entropy of micellization ( $\Delta S_{mic}$ ) of SAILs in aqueous medium at different temperatures.

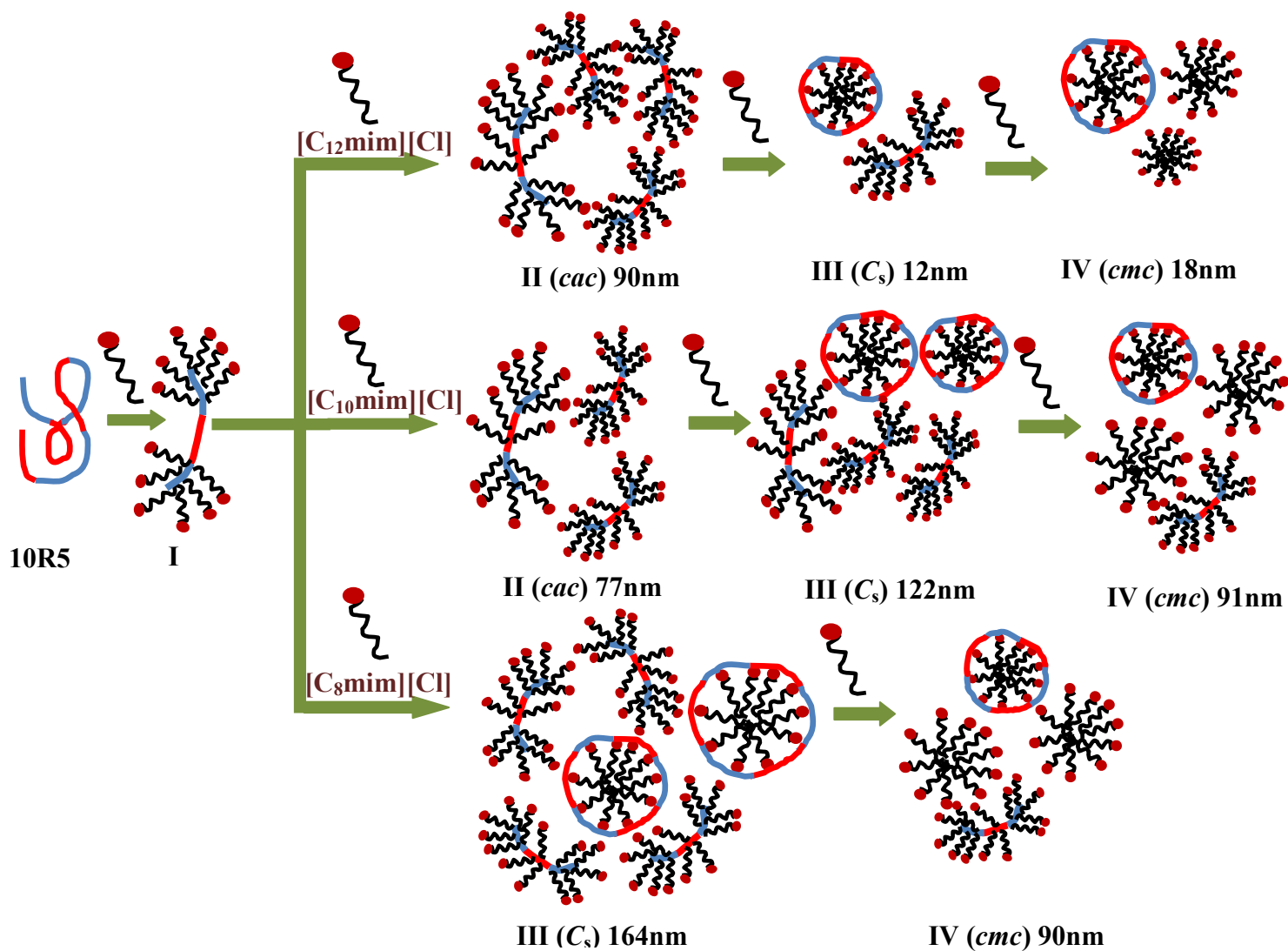
In water	T (K)	$cmc$ (mmol $dm^{-3}$ )	$\beta$	$\Delta G_{mic}$ (kJ mol $^{-1}$ )	$\Delta H_{mic}$ (kJ mol $^{-1}$ )	$\Delta S_{mic}$ (J K $^{-1}$ mol $^{-1}$ )
			[C <sub>8</sub> mim][Cl]			
	298.15	156.4	0.28	-18.6	-30.3	39.2
	303.15	161.1	0.24	-18.3	-31.3	43.0
	308.15	163.3	0.20	-17.9	-32.3	46.9
	313.15	165.7	0.18	-17.8	-33.4	49.6
	318.15	168.5	0.15	-17.6	-34.4	52.9
			[C <sub>10</sub> mim][Cl]			
	298.15	39.8	0.35	-24.2	-38.8	48.9
	303.15	40.1	0.35	-24.1	-40.1	53.1
	308.15	42.1	0.28	-23.6	-41.5	58.1
	313.15	43.8	0.25	-23.3	-42.8	62.5
	318.15	44.5	0.20	-23.2	-44.2	66.1
			[C <sub>12</sub> mim][Cl]			
	298.15	14.9	0.54	-31.4	-51.1	66.0
	303.15	15.1	0.50	-31.0	-52.8	71.8
	308.15	15.4	0.47	-30.8	-54.6	77.0
	313.15	15.7	0.43	-30.4	-56.3	82.9
	318.15	16.0	0.38	-29.8	-58.2	89.3

Table 5. Critical micelle concentration ( $cmc$ ), degree of counter ion binding ( $\beta$ ), Gibbs free energy of micellization ( $\Delta G_{mic}$ ), enthalpy of micellization ( $\Delta H_{mic}$ ) and entropy of micellization ( $\Delta S_{mic}$ ) of SAILs in polymer solution at different temperatures.

In 10R5	0.5 mmol dm <sup>-3</sup>	T (K)	$cmc$ (mmol dm <sup>-3</sup> )	$\beta$	$\Delta G_{mic}$ (kJ mol <sup>-1</sup> )	$\Delta H_{mic}$ (kJ mol <sup>-1</sup> )	$\Delta S_{mic}$ (JK <sup>-1</sup> mol <sup>-1</sup> )
[C <sub>8</sub> mim][Cl]							
		298.15	158.6	0.25	-18.2	-33.0	-49.9
		303.15	163.3	0.22	-17.9	-34.1	-53.5
		308.15	165.2	0.18	-17.6	-35.3	-57.4
		313.15	168.0	0.15	-17.4	-36.4	-60.7
		318.15	171.4	0.11	-16.9	-37.6	-64.8
[C <sub>10</sub> mim][Cl]							
		298.15	40.4	0.34	-23.8	-36.2	41.5
		303.15	41.7	0.31	-23.6	-37.4	45.6
		308.15	43.6	0.28	-23.3	-38.6	49.9
		313.15	45.1	0.26	-23.0	-39.9	54.1
		318.15	46.3	0.23	-22.5	-41.2	58.8
[C <sub>12</sub> mim][Cl]							
		298.15	15.1	0.48	-30.1	-45.5	51.7
		303.15	15.4	0.43	-29.5	-47.1	57.9
		308.15	15.5	0.40	-29.3	-48.6	62.6
		313.15	16.1	0.37	-29.1	-50.2	67.6
		318.15	16.4	0.34	-28.8	-51.8	72.4



Scheme 1.



Scheme 2.

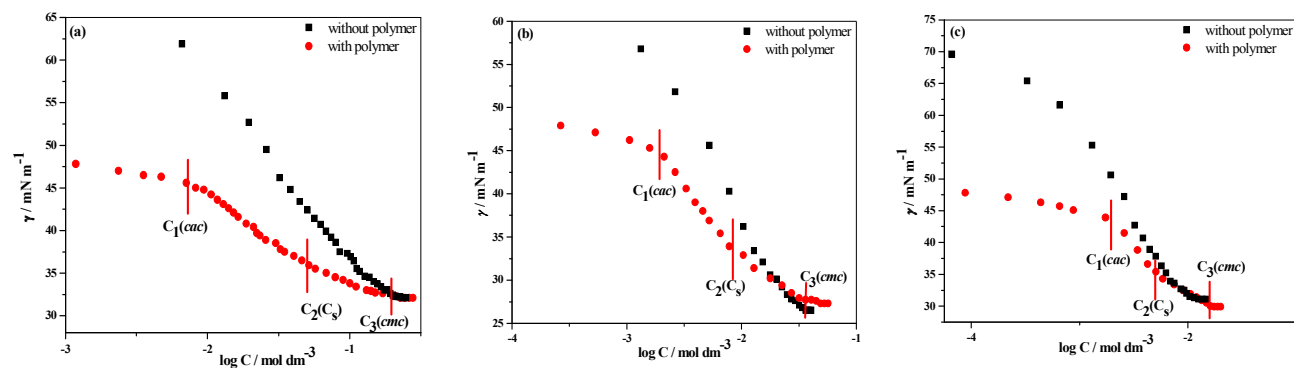


Fig. 1.

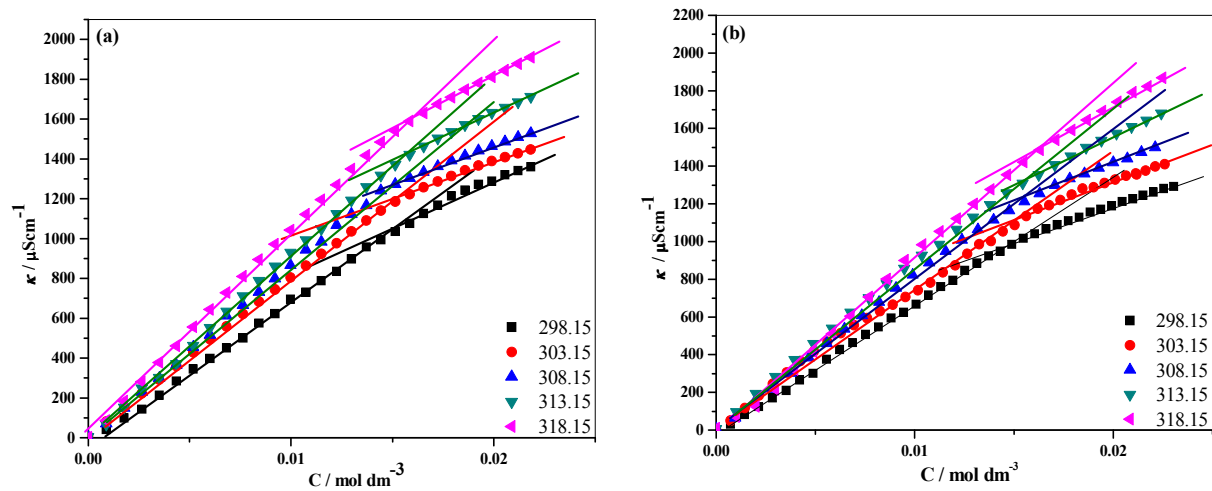


Fig. 2.

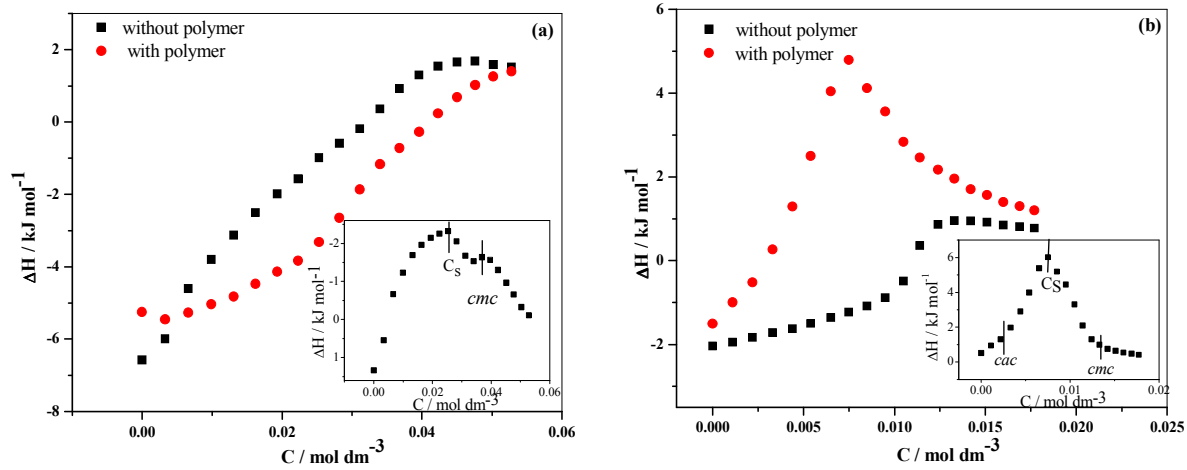


Fig. 3.

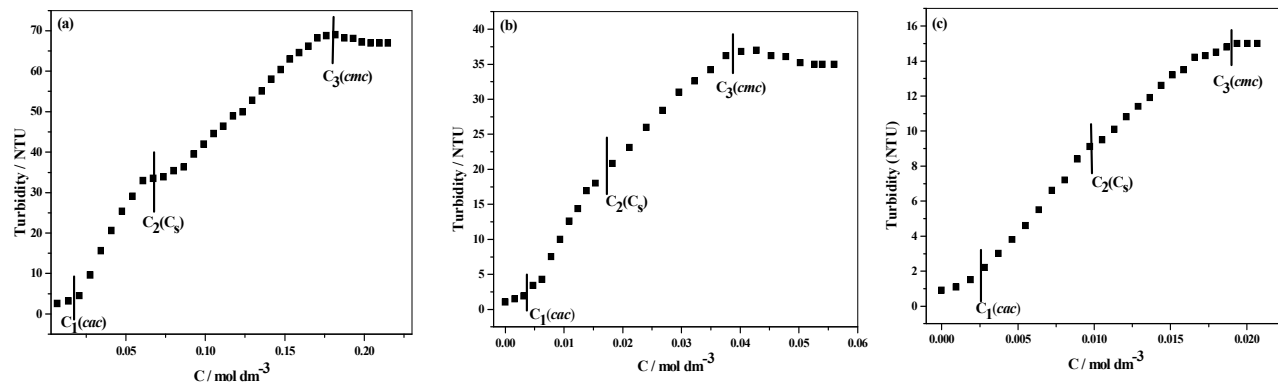


Fig. 4.

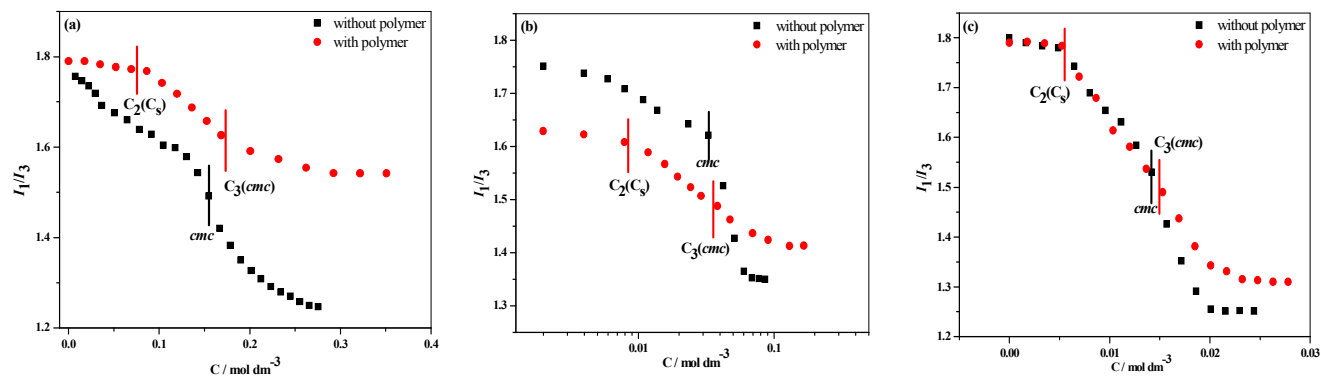


Fig. 5.

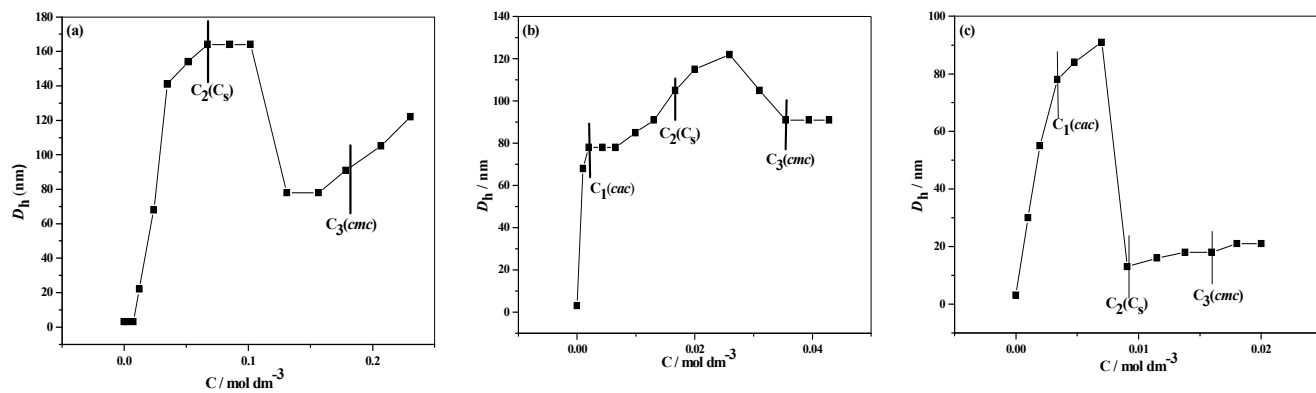


Fig. 6.